Bioorganic & Medicinal Chemistry 26 (2018) 5053–5061

Contents lists available at ScienceDirect

Bioorganic & Medicinal Chemistry

journal homepage: www.elsevier.com/locate/bmc

Andrographolide derivative as STAT3 inhibitor that protects acute liver damage in mice

Shao-Ru Chen[a,d], Feng Li[b,d], Mo-Yu Ding[a], Decai Wang[b], Qi Zhao[c], Yitao Wang[a], Guo-Chun Zhou[b,*], Ying Wang[a,*]

[a] State Key Laboratory of Quality Research in Chinese Medicine and Institute of Chinese Medical Sciences, University of Macau, Avenida da Universidade, Taipa, Macao SAR, China
[b] School of Pharmaceutical Sciences, Nanjing Tech University, Nanjing, Jiangsu 211816, China
[c] Faculty of Health Sciences, University of Macau, Avenida da Universidade, Taipa, Macao SAR, China

ARTICLE INFO

Chemical compounds cited in this article:
andrographolide (PubChem CID: 5318517)

Keywords:
Andrographolide
STAT3 inhibitor
Acute liver damage
Inflammation

ABSTRACT

Sustained activation of the Janus kinase-signal transducers and activators of transcription (JAK-STAT) pathway contributed to the progression of cancer and liver diseases. STAT3 signaling inhibitor has been extensively investigated for pharmacological use. We synthesized a series of andrographolide derivatives, and characterized their activity against STAT3 signaling pathway both in vitro and in the CCl_4-induced acute liver damage mice model. Among these derivatives, compound **24** effectively inhibited phosphorylation and dimerization of STAT3 but not its DNA binding activity. Compound **24** significantly ameliorated carbon tetrachloride-induced acute liver damage *in vivo* without changing mice body weight. Treatment with **24** attenuated hepatic pathologic damage and promoted hepatic proliferation and activation of STAT3. Compound **24** inhibited elevated expression of α-smooth muscle actin and serum pro-inflammatory cytokines downstream of STAT3 but not those factors that are regulated by NF-κB or SMADs. In summary, our results suggest that compound **24** may serve as a potential therapeutic agent for the treatment of hepatic damage or a liver protection agent via regulating STAT3 activation.

1. Introduction

Acute liver damage is a reversible wound-healing response to chemical-induced liver injury, hepatitis infection, and alcohol abuse, which will progress to chronic liver diseases such liver fibrosis and cirrhosis.[1] The farnesoid-X receptor agonist obeticholic acid has been approved for the treatment of non-cirrhotic and non-alcoholic steatohepatitis.[2] The efficacy of obeticholic acid for toxic cirrhosis has also been examined in a vertebrate model.[3] The lipid peroxidation inhibitor pentoxifylline reduced lobular inflammation in nonalcoholic steatohepatitis in clinical trials.[4] The natural products silymarin and vitamin E prevented progression of liver damage by reducing hepatic inflammation.[5] However, no medication for the treatment of liver fibrosis or acute liver damage has been approved by the Food and Drug Administration (FDA) to date.[6]

Janus kinase (JAK)-STAT pathway is one of the major pathways that regulate transcription of pro-inflammatory cytokines in acute liver damage.[7] Interferon (IFN) is essential to controlling JAK cross phosphorylation and subsequent phosphorylation of STAT1 and STAT2. Phosphorylated STAT1/2 then triggers dimerization, phosphorylation, and hence nucleus translocation of STAT3.[7] STAT3 is hyperphosphorylated in cirrhotic patients with mortality.[8,9] Sustained activation of STAT3 signaling pathway increases matricellular fibrosis and tissue tension, thereby leading to tumorigenesis in a KRAS-driven pancreatic ductal carcinoma mice model.[10] Constitutive activation of STAT3 promotes fibroblast growth factor 19 (FGF19)-triggered tumorigenesis.[11] Dimerization of STAT3 is critical to control activation and nucleus translocation of STATs.[12] Therefore, inhibition of STAT3 dimerization has significant therapeutic potential for treating liver diseases. The Src homology 2 (SH2) domain of STAT proteins are responsible for their phosphorylation and dimerization. However, the sequence of SH2 domain is of high similarity in between different STAT family members and even some oncoproteins.[13] Therefore, discovery of inhibitors with high selectivity is required to eliminate off-target effect to interfere with other signaling pathways.[7]

Andrographolide and derivatives exhibited potency in several types

* Corresponding authors.
E-mail addresses: gczhou@njtech.edu.cn (G.-C. Zhou), emilyywang@umac.mo (Y. Wang).
[d] These authors contribute equally.

https://doi.org/10.1016/j.bmc.2018.09.002
Received 11 May 2018; Received in revised form 30 August 2018; Accepted 3 September 2018
Available online 04 September 2018
0968-0896/

of inflammatory diseases, including hepatic and pulmonary fibrosis,[14,15] non-alcoholic fatty liver and steatohepatitis,[16,17] arthritis,[18] and cancer.[19] The anti-inflammatory activity of andrographolide was mainly mediated through inhibition of phosphorylation and nuclear translocation of NF-κB p65 subunit.[14,17] Andrographolide also inhibited NF-κB p65 signaling through abrogation of STAT3 phosphorylation.[20–22] However, transcription factors like NF-κB p65 play important functions in normal growth and development; therefore, specific inhibition of the STAT3 signaling rather than multiple transcription factors under disease conditions is needed.[23] Owing to the privileged structure, diverse biological activity, and low toxicity profile andrographolide offered, analogs and derivatives have been synthesized to improve its solubility and efficacy.[24]

In our previous study, we discovered that some of andrographolide analogs exhibited potent immunosuppressive activity and protected acute pulmonary infection.[25] As we are interested in expanding the scope of medicinal application of andrographolide, we reported the design, synthesis, and preliminary structure-activity-relationship (SAR) of a series of andrographolide derivatives in the current study. We discovered compound **24** as a selective inhibitor to dimerization of STAT3 and reported a detailed pharmacological evaluation of compound **24** in carbon tetrachloride (CCl_4)-induced acute liver damage in mice. We propose compound **24** as a potent STAT3 inhibitor for the protection of acute liver damage.

2. Results and discussion

2.1. Synthetic routes and physical characterization

Andrographolide derivatives were synthesized as summarized in Fig. 1. The chemical structures of all derivatives were characterized by ^{1}H NMR, ^{13}C NMR and mass spectra. The purity of each compound was determined by HPLC (Supplementary Information). In general, protection of 3, 14, or 19-OH by TBS was conducted by TBSCl-imidazole and the Ac group introduced Ac_2O catalyzed by anhydrous $ZnCl_2$.[26–30] Transformation of 3-alcohol into 3-keto was fulfilled by the oxidation of Dess-Martin periodinane (DMP) in DCM.[26–28] Selective deprotection of TBS at position 14 was achieved by TBAF in THF at −20 °C for 1 h, while selective deprotection of TBS at position 19 was achieved by TFA in DCM at −20 °C for 0.5 h. Epoxidation of 8,17-olefin was accomplished by mCPBA and $NaHCO_3$ in DCM at 0 °C or room temperature depending on starting materials. Stereochemistry of 8,17-epoxide was determined by comparing with the crystal structure of 8β,17-epoxyandrographolide and reported compounds based on spectra data and chemical transformation.[28–31]

Supplementary data associated with this article can be found, in the online version, at https://doi.org/10.1016/j.bmc.2018.09.002.

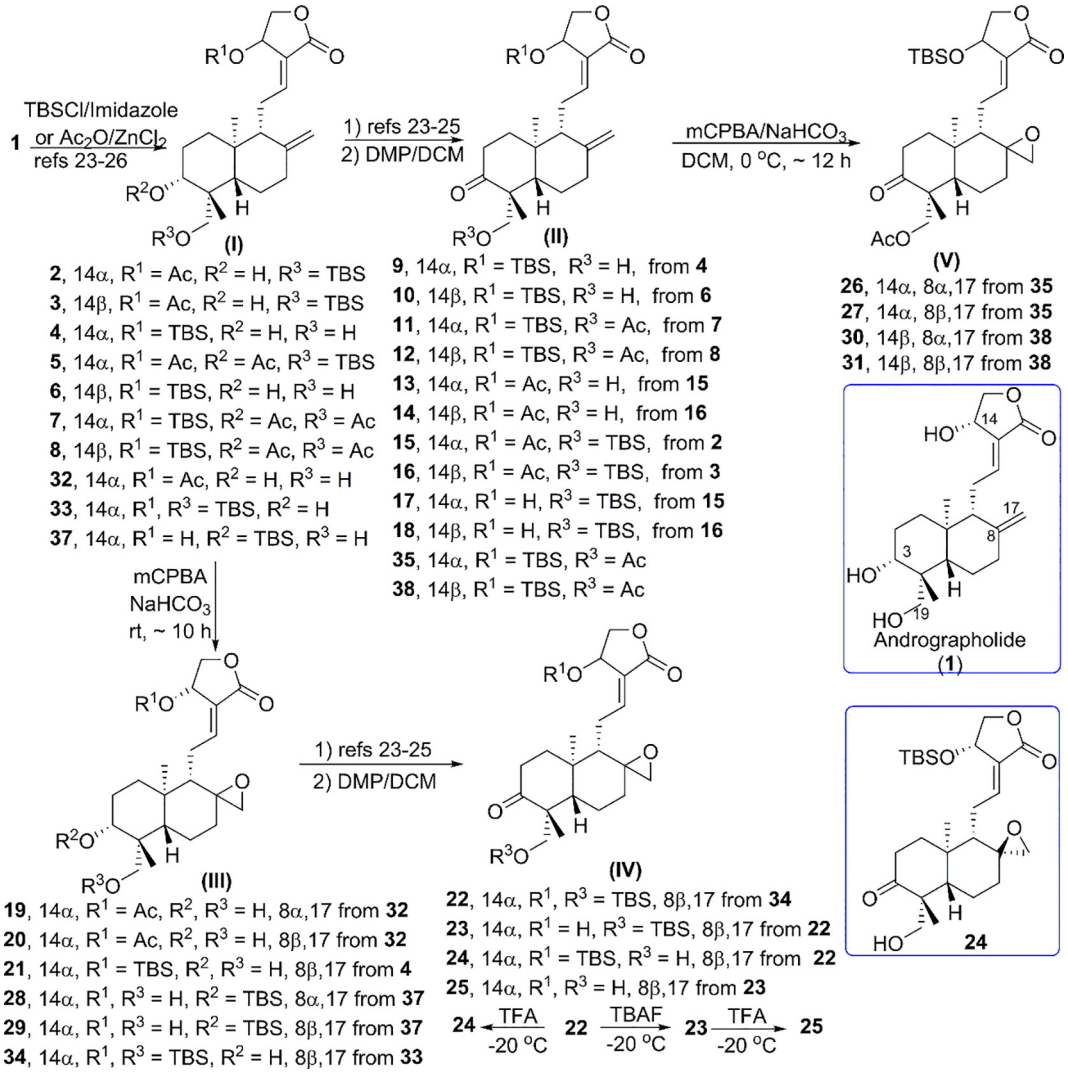

Fig. 1. Synthetic route for andrographolide analogs (DMP = Dess-Martin periodinane; mCPBA = 3-chloroperbenzoic acid).

Table 1
The EC_{50} (half effective concentration) of all compounds against IFN-γ, IL-6, and NF-κB signaling pathways and the cytotoxicity (CC_{10}, half cytotoxic concentration) in AD-293 and Hela cells.

Cmpd	AD-293 (μM)				Hela (μM)		
	IFN-γ[a]	IL-6[b]	NF-κB[c]	Cytotoxicity (CC_{10})[d]	IFN-γ[a]	NF-κB[c]	Cytotoxicity (CC_{10})[d]
1	> 10	> 10	> 10	> 10	> 10	> 10	> 10
2	1.18 ± 0.45	2.21 ± 0.68	6.92 ± 1.05	CC_{50}: 7.33 ± 0.22	4.33 ± 0.28	8.11 ± 1.65	> 10
3	8.15 ± 0.78	3.22 ± 0.42	7.28 ± 0.36	CC_{50}: 6.83 ± 0.39	9.43 ± 0.71	9.96 ± 0.65	> 10
4	5.68 ± 0.31	10.57 ± 0.19	> 10	> 10	6.57 ± 0.50	> 10	> 10
5	5.05 ± 0.59	> 10	> 10	> 10	5.80 ± 0.27	> 10	> 10
6	> 10	> 10	> 10	> 10	> 10	> 10	> 10
7	8.18 ± 0.38	> 10	> 10	> 10	> 10	> 10	> 10
8	> 10	> 10	> 10	> 10	> 10	> 10	> 10
9	> 10	> 10	> 10	> 10	> 10	> 10	> 10
10	> 10	> 10	> 10	> 10	> 10	> 10	> 10
11	> 10	> 10	> 10	> 10	> 10	> 10	> 10
12	> 10	> 10	> 10	> 10	> 10	> 10	> 10
13	7.93 ± 0.45	6.10 ± 0.32	> 10	> 10	> 10	> 10	> 10
14	> 10	> 10	> 10	> 10	> 10	> 10	> 10
15	1.97 ± 0.02	0.99 ± 0.01	7.52 ± 0.92	CC_{50} 7.35 ± 0.26	4.43 ± 0.31	4.57 ± 0.69	> 10
16	4.75 ± 0.92	4.78 ± 0.14	7.98 ± 0.51	CC_{50} 8.23 ± 0.13	9.33 ± 0.85	> 10	> 10
17	3.45 ± 1.22	6.45 ± 1.33	7.75 ± 1.02	CC_{50} 2.35 ± 0.49	8.95 ± 0.21	8.81 ± 1.11	> 10
18	4.72 ± 0.26	4.34 ± 0.03	> 10	> 10	> 10	> 10	> 10
19	2.60 ± 0.56	3.04 ± 0.52	8.51 ± 0.85	> 10	> 10	7.54 ± 1.19	> 10
20	5.11 ± 0.28	3.11 ± 0.42	9.49 ± 0.91	CC_{50}10.93 ± 1.30	9.45 ± 0.64	9.67 ± 0.31	> 10
21	3.45 ± 0.35	3.05 ± 0.49	> 10	> 10	> 10	> 10	> 10
22	4.40 ± 0.74	> 10	> 10	> 10	> 10	> 10	> 10
23	> 10	> 10	> 10	CC_{50} 8.31 ± 0.23	> 10	> 10	> 10
24	5.99 ± 0.68	3.95 ± 0.17	> 10	> 10	5.90 ± 0.38	> 10	> 10
25	> 10	> 10	> 10	> 10	> 10	> 10	> 10
26	5.81 ± 0.34	7.98 ± 0.12	> 10	> 10	> 10	> 10	> 10
27	5.38 ± 0.47	> 10	> 10	> 10	8.34 ± 0.84	> 10	> 10
28	5.39 ± 0.46	4.16 ± 0.09	> 10	> 10	6.15 ± 0.79	> 10	> 10
29	5.38 ± 0.47	> 10	> 10	> 10	8.34 ± 0.84	> 10	> 10
30	2.23 ± 0.28	2.56 ± 0.49	> 10	> 10	> 10	7.05 ± 0.64	> 10
31	2.55 ± 0.27	2.65 ± 0.64	> 10	> 10	> 10	9.91 ± 0.17	> 10

[a] Treated for 24 h.
[b] Treated for 6 h.
[c] Treated for 4 h.
[d] Treated for 24 h.

2.2. SAR against STAT3 and related signaling pathways

Pharmacological inhibition of individual STAT proteins remains challenging because of their highly similar structures.[32] We initially screened all compounds against luciferase reporters bearing STAT3 response elements with IFN-γ and IL-6 stimulation, together with reporter gene bearing NF-κB response elements to determine the specificity of the signal. Compound **1** (andrographolide) was not active against IFN-γ, IL-6, and NF-κB signaling pathways in both AD-293 and Hela cell lines at 10 μM (Table 1). The 14α- or 14β-acetylated products[26] **2** and **3** with 19-silylation inhibited all three signaling pathways, but exhibited cytotoxicity in AD-293 cells (Table 1). 14α-Silylated compound **4**[26] inhibited IFN-γ signaling pathway with moderate activity against IL-6 signaling pathway but was inactive to NF-κB signaling pathway. Compound **4** did not show obvious cytotoxicity in either cell lines (Table 1). The more lipophilic 3,14α-diacetyloxy-19-butyldimethylsilyloxy product **5**[27] was as potent as **4** against IFN-γ signaling pathway but was inactive in NF-κB or IL-6 signaling pathways. A comparison of compounds **4** and **6**[26] indicates that the 14β-butyldimethylsilyloxy resulted in a loss of activity against IFN-γ signaling pathway (Table 1), indicating the importance of 14-stereochemistry. Compounds **7**,[26] 3,19-diacetylated products of **4**, lost activity against IL-6 and IFN-γ signaling pathways. The 3,19-diacetylated product compound **8**[26] was not as potent as **6**. 3-Ketone modification products[26] of **9**, **10**, **11** and **12** were inactive against IFN-γ, IL-6, nor NF-κB signaling pathways (Table 1). 14α-Acetyloxy-3-ketone **13**[26] indicated anti-IFN-γ and anti-IL-6 signaling activity only in AD-293 cell line; but 14β-acetyloxy-3-ketone **14**[26] was totally inactive to all signaling pathways (Table 1). 14-Acetyloxy-3-ketone-19-butyldimethylsilyloxy products[26] **15** and **16** were active against IFN-γ, IL-6, and NF-κB signaling pathways with obvious cytotoxicity to AD-293 cells (Table 1). Removal of the acetyl moiety from **15** and **16** generated compound **17**[26] in the 14α configuration, which exhibited increased cytotoxicity. Compound **18**[26] in the 14β configuration attenuated IL-6 signaling and reduced cytotoxicity (Table 1). These results suggested that 14-modification and 14-stereochemistry are determinant factors to cytotoxicity.

Oxidation at positions of 8 and 17 resulted in 8α,17-epoxide **19** and 8β,17-epoxide **20**. The minor product **19** showed anti-NF-κB activity in both cell lines without cytotoxicity, and anti-IFN-γ and anti-IL-6 activities only in AD-293 cell line. However, the major product **20** was active against IFN-γ, IL-6, and NF-κB signaling pathways with a CC_{50} at 10.9 μM to AD-293 cells (Table 1). 14-Butyldimethylsilyloxy-8β,17-epoxide product **21** inhibited an IL-6 signaling pathway without cytotoxicity (Table 1). Even though 14,19-bis(butyldimethylsilyloxy)-3-ketone of 8β,17-epoxide product **22** inhibited IFN-γ signaling in AD-293 cells, 19-butyldimethylsilyloxy-3-ketone of 8β,17-epoxide product **23** was inactive in neither of the three signaling pathways and exhibited cytotoxicity to AD-293 cells (Table 1). 14-Butyldimethylsilyloxy-3-ketone of 8β,17-epoxide product **24** was active against IFN-γ signaling pathway in both cell lines, and inhibited IL-6 signaling pathway in AD-293 cells without cytotoxicity (Table 1). 14,19-Dihydroxy-3-ketone-8β,17-epoxide **25** without 14-butyldimethylsily lost activity to all the signaling pathways, suggesting that 14-butyldimethylsily and 19-free alcohol are important moieties to maintain the activity.

Compound **26** with 14-acetylation and 8α,17-epoxide exhibited

decreased anti-IL-6 signaling activity but not anti-IFN-γ signaling activity in Hela cells. However, compound **27** with 14-acetylation exhibited comparable anti-IFN-γ signaling activity to **24**, but lost anti-IL-6 signaling activity (Table 1). Interestingly, 3-butyldimethylsilyloxy-8α,17-epoxide **28** potently inhibited IFN-γ signaling pathway in both cell lines and IL-6 signaling pathway in AD-293 cell line; but 3-butyldimethyl-silyloxy-8β,17-epoxide **29** was inactive to IL-6 signaling, and only attenuated anti-IFN-γ signaling pathway activity in both cell lines (Table 1). 14β-Butyldimethylsilyloxy-19-acetyloxy-8α,17-epoxide **30** and 14β-butyldimethylsilyloxy-19-acetyloxy-8β,17-epoxide **31** exhibited anti-IL-6 signaling pathway activity, but their inhibitory activity to IFN-γ or NF-κB signaling pathways were cell line-dependent (Table 1). Combining these data revealed that compounds **4**, **24** and **28** are active against IFN-γ signaling pathway in both cell lines and active against IL-6 signaling in AD-293 cells, but was not active against NF-κB signaling pathway in either cell lines. Compound **19** is active against NF-κB signaling pathway, and compounds **5**, **27** and **29** are active against IFN-γ signaling pathway in both cell lines and not active against IL-6 and NF-κB signaling pathways.

2.3. Compound *24* specifically inhibited phosphorylation and dimerization of STAT3

To further confirm the inhibitory effect of the active characteristic, we measured the impact of compounds **4**, **5**, **24**, **27**, **28** and **29** on STAT1 and STAT3 by Western blotting (Fig. 2A-C). Compounds **4** and **5** did not change IFN-γ (1.0 μg/mL)-stimulated expression of STAT1 and STAT3 (Fig. 2A-C), whereas compound **27** suppressed the expression and phosphorylation of STAT3 (Fig. 2A-C). Compounds **28** and **29** did not affect the expression and phosphorylation of STAT1 nor STAT3 (Fig. 2A-C). Compound **24** specifically blocked expression of phosphorylated STAT3 to more than 50% compared to DMSO-treated control but did not affect expression and phosphorylation of STAT1 (Fig. 2A-C). These results suggest that compound 24 specifically inhibited STAT3 but not STAT1.

The dimerization of STAT3 controls its phosphorylation and nucleus translocation, and thus is regarded as an important therapeutic target.[33] We then transiently transfected GFP- and FLAG-tagged STAT3 plasmids into AD-293 cells, and determined the interaction of GFP-STAT3 and FLAG-STAT3 by immunoprecipitation. Compound **24** decreased interactions of GFP-STAT3 and FLAG-STAT3 monomers at 10 μM concentration (Fig. 2D), which is close to the anti-Stat3 activity of Stattic (IC_{50} = 5.1 μM)[7] and higher than that of S3I-201 (IC_{50} = 86 μM).[34] Phosphorylation and dimerization triggers nucleus translocation of STAT3, and hence promotes the biding to its specific DNA motifs and hence trigger transcription.[35] Compound **24** did not affect the DNA binding activity of STAT3 for up to 40 μM (Fig. 2E); while the addition of three times free oligo reduced DNA binding activity (Fig. 2E).

2.4. Compound *24* protected CCl_4-induced acute liver damage

Sustained phosphorylation of STAT3 triggered liver fibrosis and damage in ethanol-fed and CCl_4-treated mice.[36,37] Despite the important function of activated STAT3 in promoting pathogenesis in liver damage, only a few STAT3 inhibitors have been tested in liver damage models. Sorafenib, an oral multi-kinase inhibitor and the only FDA approved drug for HCC, exhibited anti-fibrotic activity through decreasing accumulation of collagen in hepatic stellate cells (HSC).[38] Treatment with STAT3 inhibitor S3I-201 ameliorated renal interstitial fibrogenesis in obstructive nephropathy,[39] and is currently in phase I clinical trials for the malignant glioma and brain metastasis derived from melanoma.[40] Therefore, we challenged mice with CCl_4 to mimic acute liver damage. Mice did not indicate a significant change in body weight after treatment with CCl_4 alone or in combination with oral

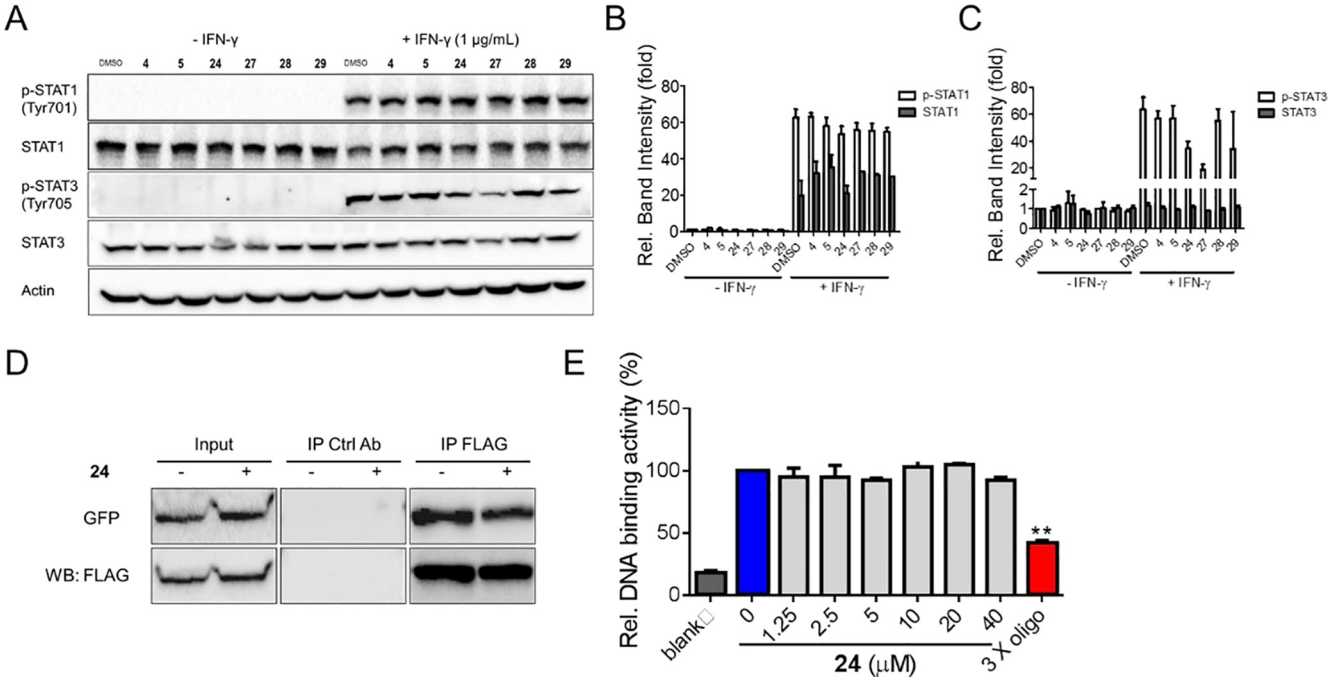

Fig. 2. Compound **24** inhibited dimerization of STAT3 in AD-293 cells. (A) Effect of compounds **4**, **5**, **24**, **27**, **28**, and **29** on IFN-γ-stimulated phosphorylation of STAT1 and STAT3. AD-293 cells were treated with 1 μg/mL IFN-γ alone or in the presence of compounds at 10 μM. Expression levels of phosphorylated-STAT1 and STAT3, and total STAT1 and STAT3 in whole-cell lysates were examined by Western blot analysis. The blot of actin was used as internal loading control. Quantification of (B) phosphorylated STAT1 and STAT1 levels, and (C) phosphorylated STAT3 and STAT3 levels. (D) AD-293 cells were co-transfected with FLAG-tagged and GFP-tagged STAT3 plasmids and treated with IFN-γ alone or in the presence of compound **24** for 6 h. Cells were harvested and the association of FLAG-tagged and GFP-tagged STAT3 were analyzed by co-immunoprecipitation assay followed by western blot analysis. (E) Effect of compound **24** on the DNA binding activity of STAT3 using TransAM STAT Family Kit. 3X oligo is the results of DNA binding activity in the presence of three times free oligo. The results were representative of at least three independent experiments. Results in (E) are presented as mean ± SD from three separate experiments (**, $p < 0.05$).

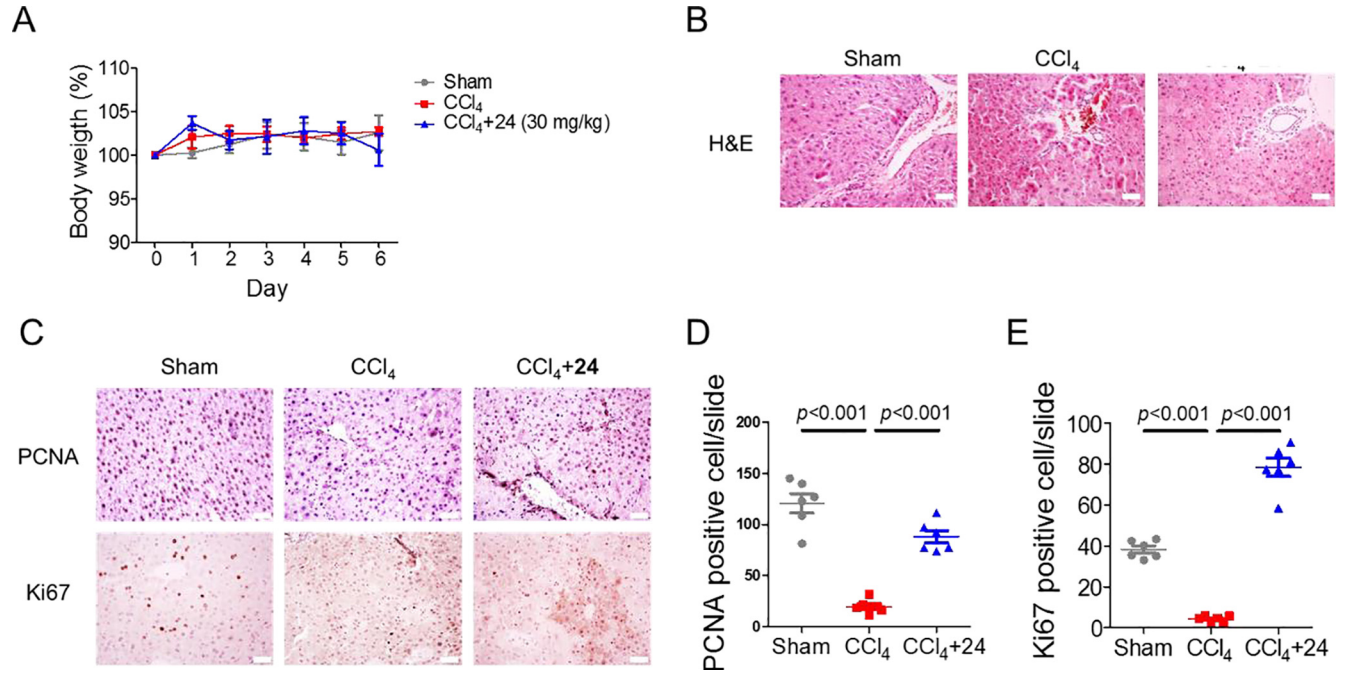

Fig. 3. Compound **24** protected liver damage in CCl_4-induced acute liver damage mice. (A) Body weight changes of BalB/C mice during the treatment. Error bars indicate S.E.M. (B) H&E staining of paraffin fixed liver sections from samples collected 16 h after CCl_4 injection. Scale bar, 200 μm. (C) PCNA and Ki67 staining per liver section at the end of the treatment. Quantitative results of (D) PCNA and (E) Ki67 staining. Details of experimental procedures are given in the Materials and Methods section. The results were representative from two independent experiments (n = 5). *P* values are as indicated in the figure.

administration of compound **24** at 30 mg/kg (Fig. 3A). Liver sections from CCl_4-treated mice indicated hepatic damage and increased numbers of necrotic cells as indicated by H&E staining (Fig. 3B). Mice treated with **24** exhibited significant histological improvement (Fig. 3B). Liver proliferation activity was estimated by the number of proliferating cell nuclear antigen (PCNA) and Ki67-positive cells per view of liver sections (Fig. 3C). Compound **24** significantly increased PCNA- and Ki67-positive cell numbers compared with CCl_4 treatment (Fig. 3C), thereby suggesting that compound **24** was able to increase DNA replication and cell proliferation in chemical-induced acute liver damage.

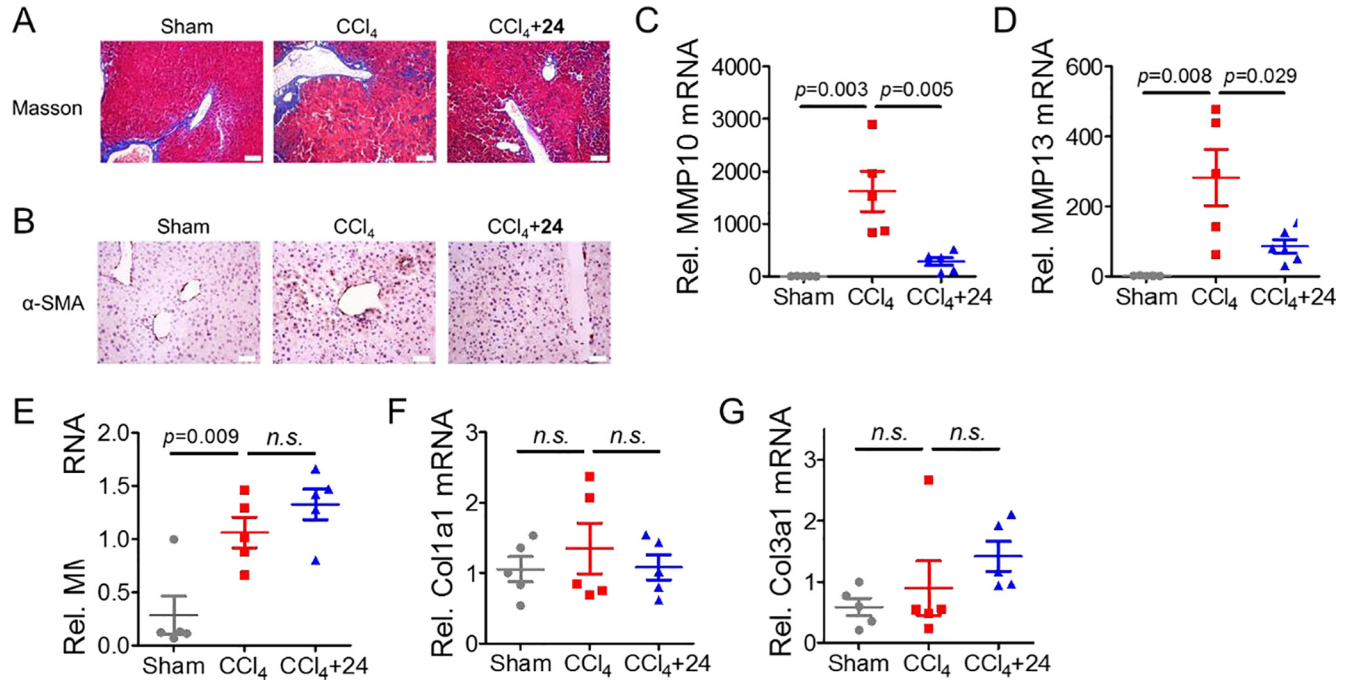

Fig. 4. Compound **24** reduced expression levels of factors that promote liver damage and fibrosis. (A) Masson staining of paraffin fixed liver sections from samples collected 16 h after CCl_4 injection. (B) α-SMA staining per liver section at the end of the treatment. Scale bar, 200 μm. mRNA levels of (C) MMP10, (D) MMP13, (E) MMP9, (F) Col1a1, and (G) Col3a1 in the liver at the end of the treatment. Results were representative from two independent experiments (n = 5). Details of experimental procedures are given in Materials and Methods. *P* values are as indicated in the figure.

2.5. Compound **24** attenuated expression of genes that promote liver damage and fibrosis in CCl_4-induced acute liver damage in vivo

The liver can rapidly activate tissue regeneration and immunity in response to acute damage.[41] Persistent activation of inflammatory response leads to fibrosis and cirrhosis.[41] Therefore, we analyzed key factors that promote hepatic fibrogenesis. Increased blue stained areas in Masson's trichrome staining revealed the formation of collagen in CCl_4 treatment (Fig. 4A). Compound **24** treatment decreased collagen formation as indicated by Masson's trichrome staining (Fig. 4A). Compound **24** also suppressed CCl_4 treatment-induced expression of α-SMA in the areas surrounding blood vessel (Fig. 4B). We then examined transcription of matrix metallopeptidases (MMPs) that were regulated by different transcriptional factors. The highly increased mRNA levels of MMP10 and MMP13 with CCl_4-treatment, which were regulated by JAK signaling pathway,[42,43] were significantly attenuated by compound **24** (Fig. 4C-D). Compound **24** failed to suppress CCl_4-treatment-induced upregulation of transcription of MMP9 (Fig. 4E). In addition, the transcriptions of collagen type I α1 chain (Col1a1) and Col3a1 remained unchanged (Fig. 4F-G). Compound **24** did not significantly reduce CCl_4-induced elevated serum ALT and AST levels (results not shown).

2.6. Compound **24** inhibited STAT3 activation in CCl_4-induced acute liver damage in vivo

To further determine whether compound **24** could inhibit STAT3 signaling in CCl_4-induced acute liver damage mice, we determined the expression level of STAT3 and downstream factors *in vivo* (Fig. 5). Immunohistochemistry results revealed that compound **24** significantly decreased CCl_4-induced expression of STAT3 (Fig. 5A-B). STAT3 was predominantly located in the nucleus in CCl_4-treated mice, which indicates that STAT3 was in the active phosphorylated state. The number of cells with positive nucleus staining of STAT3 were significantly decreased in mice with compound **24** treatment (Fig. 5A-B). We then determined pro-inflammatory cytokine and chemokine level in the serum. Among all the pro-inflammatory cytokines and chemokines detected, the levels of IL-6, MCP-1, and TGF-β were significantly downregulated by compound **24** (Fig. 5C-E). Our results are in line with previous report that noncanonical STAT3 activation also governs the excess production of TGF-β and collagen I, and the formation of intestinal fibrosis in muscles of Crohn's disease.[44] By contrast, compound **24** was unable to decrease CCl_4-treatment induced mRNA expressions of SMAD2, SMAD3, and SMAD4 (Fig. 5F-H). Compound **24** did not suppress more than 50% of SMAD2/3 reporter activity with even up to 10 μM concentration in AD-293 cells bearing promoter region of SMAD2/3 (Fig. 5J).

3. Conclusion

Here, we reported diverse modified andrographolide derivatives. The SAR indicated that 14-modification and 14-stereochemistry are determinant factors to cytotoxicity, whereas 14-butyldimethylsil and 19-free alcohol are important moieties for maintaining the activity. In this study, we found that compounds **4**, **5**, **24**, **27**, **28**, and **29** are active against IFN-γ signaling pathway in AD-293 and HeLa cell lines, whereas **4**, **24**, and **28** are also active against IL-6 signaling pathways. Andrographolide derivatives **4**, **5**, **24**, **27**, **28**, and **29** are structurally different from oligonucleotide and other small molecule STAT inhibitors, and exhibit potent inhibitory activity against STAT signaling pathways. Our study provided evidence that inhibiting STAT3 activation by andrographolide derivative was effective against chemical-induced acute liver damage. This series of compounds are structurally different from other STAT3 inhibitors. Despite the increased selectivity against STAT3, the inhibitory activity of compound **24** was actually decreased compared with other derivatives (Table 2 and Fig. 2). Therefore, compound **24** could be used as a scaffold to be developed from the broadly used natural product as active STAT3 inhibitor that maintain both selectivity and inhibitory activity in the clinic.

4. Materials and methods

4.1. General information for chemistry

^1H and ^{13}C NMR spectra were recorded on a Bruker AV-400 spectrometer at 400 and 101 MHz, respectively. Coupling constants (J) are expressed in hertz (Hz). Chemical shifts of NMR are reported in parts per million (ppm) units relative to the solvent. The high resolution of MS (HRMS) was recorded on an Applied Biosystems Q-STAR Elite ESI-LC-MS/MS mass spectrometer. Melting points were measured using YRT-3 melting point apparatus (Shanghai, China) and were

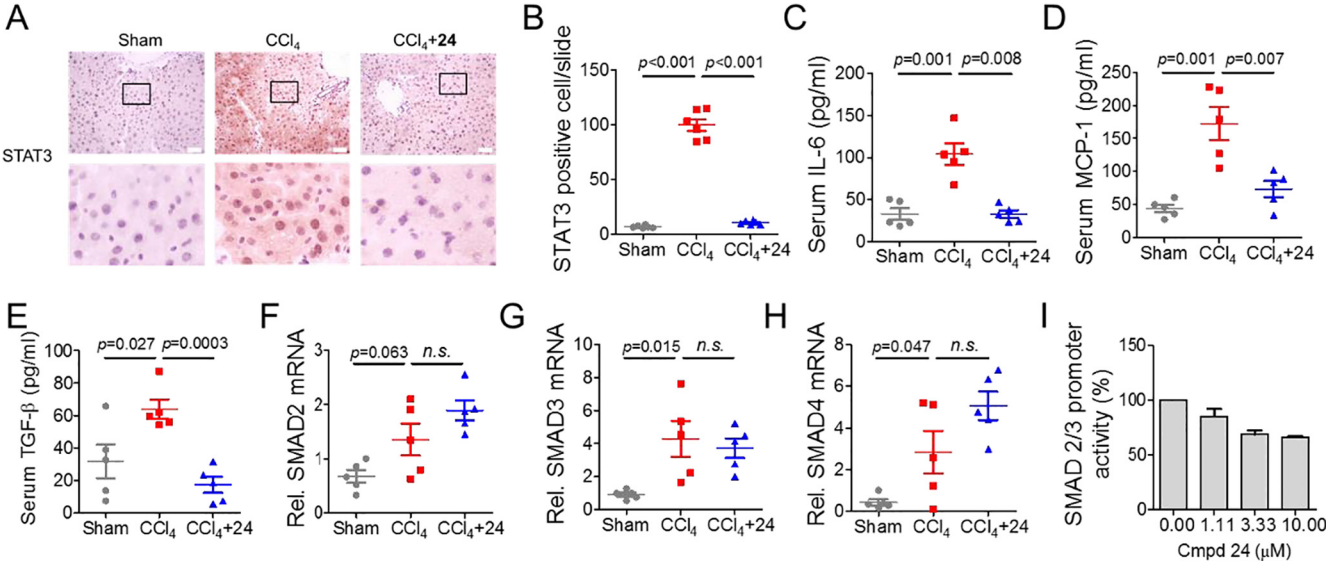

Fig. 5. Compound **24** inhibited CCl_4-induced inflammation and STAT3 activation in acute liver damage mice. (A) STAT3 per liver section at the end of the treatment. Scale bar, 200 μm. (B) Quantitative result of STAT3 staining. Serum (C) IL-6, (D) MCP-1, and (E) TGF-β level at the end of the treatment. mRNA levels of (F) SMAD2, (G) SMAD3, and (H) SMAD4 in the liver. (J) Effect of compound **24** on TGF-β-induced changes of SMAD 2/3 promoter. Results were representative from two independent experiments (n = 5). Details of experimental procedures are given in Materials and Methods. *P* values are as indicated in the figure.

Table 2
Primer sequences for real-time PCR analysis.

Gene (Gene ID)	Forward primer (5′-3′)	Reverse primer (5′-3′)
Mmp9	GCAGAGGCATACTTGTACCG	TGATGTTATGATGGTCCCACTTG
Mmp10	GGACCCGAAGCGGACATTG	CGTCGTCGAAATGGGCATCT
Mmp13	CTTCTTCTTGTTGAGCTGGACTC	CTGTGGAGGTCACTGTAGACT
Col1a1	GCTCCTCTTAGGGGCCACT	CCACGTCTCACCATTGGGG
Col3a1	CTGTAACATGGAAACTGGGGAAA	CCATAGCTGAACTGAAAACCACC
Smad2	ATGTCGTCCATCTTGCCATTC	AACCGTCCTGTTTTCTTTAGCTT
Smad3	CACGCAGAACGTGAACACC	GGCAGTAGATAACGTGAGGGA
Smad4	AGCCGTCCTTACCCACTGAA	GGTGGTAGTGCTGTTATGATGGT
Gapdh	AGGTCGGTGTGAACGGATTTG	TGTAGACCATGTAGTTGAGGTCA

uncorrected. Compounds **2–4** and **6–18** were published previously by our laboratory.[26] The purity of these compounds in this report except compound **26** (about 96.4% in purity) is higher than 98%. ^{1}H NMR and ^{13}C NMR spectra of new compounds appear in SI and HPLC spectra of all compounds appear are provided in Supplementary Information.

4.2. Materials and reagents

Cell culture media, penicillin streptomycin, and fetal bovine serum (FBS) were purchased from Gibco (Carlsbad, CA, USA). Interferon-γ (IFN-γ), IL-6, and tumor necrosis factor (TNF)-α were purchased from PeproTech (Rocky Hill, NJ, USA). CCl_4 and all other reagents were purchased from Sigma-Aldrich (St. Louis, MO, USA) without further purification except noted otherwise.

4.3. Cell culture condition

Cell lines were obtained from the American Type Culture Collection (ATCC). HeLa and AD-293 cells were maintained in DMEM high glucose medium supplemented with 10% FBS and 1% penicillin streptomycin. Hela and AD-293 stable cell lines harboring IFN-γ, IL-6, and TNF-α/NF-κB response elements in pGL4.20 vector (Promega, Madison, WI, USA) were maintained in the presence of 1 μg/mL puromycin.

4.4. Signaling pathway reporter assay

Hela and AD-293 cell lines stably harboring luciferase reporter plasmids with promoter regions of IFN-γ, IL-6, and NF-κB were used for the signaling pathway reporter assay (manuscript accepted for publication). Cells were treated with 20 pg/mL IFN-γ, 2.5 μg/mL IL-6, or 50 ng/mL TNF-α to stimulate the corresponding downstream signaling pathways, respectively. SMAD2/3 promoter was inserted into the pGL4.20 vector, and stimulated with TGF-β at 100 ng/ml for 16 h. At the end of the treatment, cell extracts were prepared and luciferase activity was measured by Luciferase assay kit (Promega) according to the manufacturer's instructions.

4.5. Western blot analysis

Western blot analysis was done using primary antibodies against phosphorylated STAT1 (#7649, Cell Signaling Technology, Boston, MA, USA), phosphorylated STAT3 (#9145, Cell Signaling Technology), STAT1 (#9172, Cell Signaling Technology), STAT3 (#4904, Cell Signaling Technology), GFP (#sc-9996, Santa Cruz, Dalla, TX, USA), and actin (#A5316, Sigma-Aldrich) at optimal dilution.

4.6. Co-immunoprecipitation assay

AD-293 cells were co-transfected with pCMV6-AC-STAT3-GFP (OriGene, Rockville, MD, USA) and pRc/CMV-STAT3-FLAG (Addgene, Cambridge, MA, USA) with Turbo transfection reagent (Life Technologies, Carlsbad, CA, USA) for 48 hours[45] Cells were treated with IFN-γ alone or together with compound **24** for an additional 6 h. After cells were lysed in RIPA lysis buffer, 100 μg of each protein sample was subjected to immunoprecipitation with anti-FLAG M2 antibody (#F1804, Sigma-Aldrich) and protein G magnetic beads (Life Technologies). The purified protein-antibody complex was subjected to SDS-PAGE and Western blot. The samples were then detected with anti-GFP antibody and anti-FLAG antibody and visualized with chemiluminescent reagent (GE Healthcare, Waukesha, WI, USA).

4.7. STAT3 DNA binding activity

STAT3 DNA binding activity was determined using the TransAM STAT family kit from Active Motif's following the manufacture's recommendation.

4.8. Animals

Male WT BalB/C mice were obtained from Animal Facility at University of Macau. All methods were carried out in accordance with relevant guidelines and regulations. All experimental protocols were approved by the Animal Research Ethics Committee at University of Macau. Mice (20–25 g, 6–8 weeks old) were acclimated for 1 week prior to use in experiments and were allowed free access to water and chow diet through the experiment. In vivo experiments were performed in the animal facility.

4.9. Treatment conditions

Experimental animals were given compound **24** (30 mg/kg) orally once daily for 7 days before subcutaneous injection of CCl_4 (40% CCl_4 in olive oil, 10 ml/kg body weight). Mice were sacrificed 16 h after CCl_4 injection. Control mice were injected with an equivalent amount of corn oil subcutaneously. Mice were sacrificed after being anaesthetized with CO_2. Serum was collected and stored at −70 °C until analysis. Liver was removed, washed with ice cold PBS (pH 7.4), and fixed by 10% formaldehyde solution for histologic analysis or stored at −70 °C for RNA extraction.

4.10. Histological analysis

After fixation, dehydration, and antigen retrieval, liver section was stained with haematoxylin and eosin (H&E) staining solution and masson's trichrome staining (Nanjing Jiancheng Bioengineering Institute, Nanjing, China), and examined under light microscopy. At least three different sections were examined per liver.

4.11. Immunohistochemistry

Paraffin fixed liver sections were fixed, and washed by PBS before block with 3% H_2O_2 solution. Liver sections were then washed by TBS-T and blocked in blocking buffer containing 10% goat serum, 0.1% BSA, 0.2% gelatin at room temperature for 1 h. Liver sections were then incubated in primary antibody against PCNA (#2586, Cell Signaling Technology), Ki67 (#ab15580, Abcam, Cambridge, UK), STAT3 (#ab68153, Abcam), and α-smooth muscle actin (α-SMA, #ab5694, Abcam) in blocking buffer at 4 °C overnight, washed by TBS-T and then incubated with HRP-conjugated secondary antibody. A set of slides were processed without incubation with primary antibody as negative control. The signal was detected by DAB peroxidase substrate kit (Vector Laboratories, Burlingame, CA, USA). The slides were counter-stained with hematoxylin and mounted. To quantify stains of different proteins, pictures were taken of > 30 fields of view at 400× magnification. Adobe Photoshop CS6 software was used to pixel count the positive staining. The stains were scored by three researchers separately in blind.

4.12. Measurement of serum pro-inflammatory cytokine and chemokine

Serum pro-inflammatory cytokine and chemokine levels were determined using BioLegend LEGENDplex™ kits (BioLegend, San Diego, CA, USA) according to the manufacture's recommendations.

4.13. RNA isolation and quantitative real-time PCR

Total RNA from liver was isolated using Trizol® reagent (Invitrogen). cDNA was synthesized from total RNA using random primers and iScript™ cDNA synthesis kit (Bio-Rad Laboratories, Hercules, CA, USA) Expression levels of specific genes were quantified by real-time PCR using SYBR Green Master Mix (Bio-Rad Laboratories). The primer sequences were listed in Table 2.

4.14. Statistical analysis

Data are presented as mean ± S.D. or mean ± S.E.M. No animals were excluded for analysis. All experiments were repeated two or more times. Data were normally distributed, and the variance between groups was not significantly different. Differences in measured variables between groups were analyzed by one-way or two-way ANOVA, or the student's t test by GraphPad Prism 5 software. Results were considered statistically significant when $p < 0.05$.

5. Author contributions

GCZ and YW conceived and supervised the project, analyzed the data and wrote the paper. GCZ, FL and DW designed the andrographolide derivatives, FL and DW conducted the syntheses of andrographolide derivatives. YW, SRC, MYD, QZ, and YTW designed the experiments. SRC and QZ conducted the biology experiments. All authors have read and approved the final manuscript.

Acknowledgement

The authors thank Prof. Chuang-Hang Leung and Ms. Li-Juan Liu for the pCMV6-AC-STAT3-GFP and pRc/CMV-STAT3-FLAG plasmids, and Yuran Peng for technical assistant. This work was partially supported by Research Fund of the University of Macao MYRG2016-00105-ICMS-QRCM, and MYRG2017-00116-ICMS-QRCM to YW. This work was partially supported by Natural Science Foundation of China (U0632001) and Six Major Talents of Jiangsu Province of China (2014) to GCZ.

Conflict of interest

The authors declare no conflict of interest.

References

1. Chen SR, Chen XP, Lu JJ, Wang Y, Wang YT. Potent natural products and herbal medicines for treating liver fibrosis. *Chin Med.* 2015;10:7.
2. Neuschwander-Tetri BA, Loomba R, Sanyal AJ, et al. Farnesoid X nuclear receptor ligand obeticholic acid for non-cirrhotic, non-alcoholic steatohepatitis (FLINT): a multicentre, randomised, placebo-controlled trial. *Lancet.* 2015;385:956–965.
3. Verbeke L, Mannaerts I, Schierwagen R, et al. agonist obeticholic acid reduces hepatic inflammation and fibrosis in a rat model of toxic cirrhosis. *Sci Rep.* 2016;6:33453.
4. Zein CO, Yerian LM, Gogate P, et al. Pentoxifylline improves nonalcoholic steatohepatitis: a randomized placebo-controlled trial. *Hepatology.* 2011;54:1610–1619.
5. Loguercio C, Andreone P, Brisc C, et al. Silybin combined with phosphatidylcholine and vitamin E in patients with nonalcoholic fatty liver disease: a randomized controlled trial. *Free Radical Biol Med.* 2012;52:1658–1665.
6. Ding N, Yu RT, Subramaniam N, et al. A vitamin D receptor/SMAD genomic circuit gates hepatic fibrotic response. *Cell.* 2013;153:601–613.
7. Schust J, Sperl B, Hollis A, Mayer TU, Berg T. Stattic: a small-molecule inhibitor of STAT3 activation and dimerization. *Chem Biol.* 2006;13:1235–1242.
8. Ikeda A, Shimizu T, Matsumoto Y, et al. Leptin receptor somatic mutations are frequent in HCV-infected cirrhotic liver and associated with hepatocellular carcinoma. *Gastroenterology.* 2014;146:222–232 e235.
9. Zhou D, Springer MZ, Xu D, et al. Small molecules inhibit STAT3 activation, autophagy, and cancer cell anchorage-independent growth. *Bioorg Med Chem.* 2017;25:2995–3005.
10. Laklai H, Miroshnikova YA, Pickup MW, et al. Genotype tunes pancreatic ductal adenocarcinoma tissue tension to induce matricellular fibrosis and tumor progression. *Nat Med.* 2016;22:497–505.
11. Zhou M, Yang H, Learned RM, Tian H, Ling L. Non-cell-autonomous activation of IL-6/STAT3 signaling mediates FGF19-driven hepatocarcinogenesis. *Nat Commun.* 2017;8:15433.
12. Su TH, Shiau CW, Jao P, et al. Sorafenib and its derivative SC-1 exhibit antifibrotic effects through signal transducer and activator of transcription 3 inhibition. *PNAS.* 2015;112:7243–7248.
13. Zhou Q, Zhu J, Chen J, Ji P, Qiao C. N-Arylsulfonylsubstituted-1H indole derivatives as small molecule dual inhibitors of signal transducer and activator of transcription 3 (STAT3) and tubulin. *Bioorg Med Chem.* 2018;26:96–106.
14. Yin JN, Li YN, Gao Y, Li SB, Li JD. Andrographolide plays an important role in bleomycin-induced pulmonary fibrosis treatment. *Int J Clin Exp Med.* 2015;8:12374–12381.
15. Lee TY, Chang HH, Wen CK, Huang TH, Chang YS. Modulation of thioacetamide-induced hepatic inflammations, angiogenesis and fibrosis by andrographolide in mice. *J Ethnopharmacol.* 2014;158 Pt A:423–430.
16. Toppo E, Darvin SS, Esakkimuthu S, et al. Effect of two andrographolide derivatives on cellular and rodent models of non-alcoholic fatty liver disease. *Biomed Pharmacother.* 2017;95:402–411.
17. Cabrera D, Wree A, Povero D, et al. Andrographolide ameliorates inflammation and fibrogenesis and attenuates inflammasome activation in experimental non-alcoholic steatohepatitis. *Sci Rep.* 2017;7:3491.
18. Laev SS, Salakhutdinov NF. Anti-arthritic agents: progress and potential. *Bioorg Med Chem.* 2015;23:3059–3080.
19. Belal A, El-Gendy Bel D. Pyrrolizines: promising scaffolds for anticancer drugs. *Bioorg Med Chem.* 2014;22:46–53.
20. Lee KC, Chang HH, Chung YH, Lee TY. Andrographolide acts as an anti-inflammatory agent in LPS-stimulated RAW264.7 macrophages by inhibiting STAT3-mediated suppression of the NF-kappaB pathway. *J Ethnopharmacol.* 2011;135:678–684.
21. Bao GQ, Shen BY, Pan CP, Zhang YJ, Shi MM, Peng CH. Andrographolide causes apoptosis via inactivation of STAT3 and Akt and potentiates antitumor activity of gemcitabine in pancreatic cancer. *Toxicol Lett.* 2013;222:23–35.
22. Ambili R, Janam P, Saneesh Babu PS, et al. ex vivo evaluation of the efficacy of andrographolide in modulating differential expression of transcription factors and target genes in periodontal cells and its potential role in treating periodontal diseases. *J Ethnopharmacol.* 2017;196:160–167.
23. Zhang Q, Lenardo MJ, Baltimore D. 30 years of NF-kappaB: a blossoming of relevance to human pathobiology. *Cell.* 2017;168:37–57.
24. Tan WSD, Liao W, Zhou S, Wong WSF. Is there a future for andrographolide to be an anti-inflammatory drug? Deciphering its major mechanisms of action. *Biochem Pharmacol.* 2017;139:71–81.
25. Nie X, Chen SR, Wang K, et al. Attenuation of innate immunity by andrographolide derivatives through NF-kappaB signaling pathway. *Sci Rep.* 2017;7:4738.
26. Peng YR, Li JJ, Sun YC, et al. SAR studies of 3,14,19-derivatives of andrographolide on anti-proliferative activity to cancer cells and toxicity to zebrafish: an in vitro and in vivo study. *RSC Adv.* 2015;5:22510–22526.
27. Sirion U, Kasemsook S, Suksen K, Piyachaturawat P, Suksamrarn A, Saeeng R. New substituted C-19-andrographolide analogues with potent cytotoxic activities. *Bioorg Med Chem Lett.* 2012;22:49–52.
28. Yicheng YS Peng, Decai Wang, Pingkai Ouyang, Guo-Chun Zhou. Synthesis of 8,17-epoxide-andrographolide derivatives and screening their antibacterial activity. *J Nanjing Tech Univ (Natural Science Ed).* 2016:67–78.
29. Xu HW, Dai GF, Liu GZ, Wang JF, Liu HM. Synthesis of andrographolide derivatives: a new family of alpha-glucosidase inhibitors. *Bioorg Med Chem.* 2007;15:4247–4255.
30. Nanduri S, Nyavanandi VK, Thunuguntla SSR, et al. Synthesis and structure-activity relationships of andrographolide analogues as novel cytotoxic agents. *Bioorg Med Chem Lett.* 2004;14:4711–4717.
31. Preet R, Chakraborty B, Siddharth S, et al. Synthesis and biological evaluation of andrographolide analogues as anti-cancer agents. *Eur J Med Chem.* 2014;85:95–106.
32. Furqan M, Akinleye A, Mukhi N, Mittal V, Chen Y, Liu D. STAT inhibitors for cancer therapy. *J Hematol Oncol.* 2013;6:90.
33. Ioannidis S, Lamb ML, Wang T, et al. Discovery of 5-chloro-N2-[(1S)-1-(5-fluoropyrimidin-2-yl)ethyl]-N4-(5-methyl-1H-pyrazol-3-yl)p yrimidine-2,4-diamine (AZD1480) as a novel inhibitor of the Jak/Stat pathway. *J Med Chem.* 2011;54:262–276.
34. Siddiquee K, Zhang S, Guida WC, et al. Selective chemical probe inhibitor of Stat3, identified through structure-based virtual screening, induces antitumor activity. *PNAS.* 2007;104:7391–7396.
35. Daka P, Liu A, Karunaratne C, et al. Design, synthesis and evaluation of XZH-5 analogues as STAT3 inhibitors. *Bioorg Med Chem.* 2015;23:1348–1355.
36. Kwon HJ, Won YS, Park O, et al. Aldehyde dehydrogenase 2 deficiency ameliorates alcoholic fatty liver but worsens liver inflammation and fibrosis in mice. *Hepatology.* 2014;60:146–157.
37. Liu Y, Shao M, Wu Y, et al. Role for the endoplasmic reticulum stress sensor IRE1alpha in liver regenerative responses. *J Hepatol.* 2015;62:590–598.
38. Deng YR, Ma HD, Tsuneyama K, et al. STAT3-mediated attenuation of CCl4-induced mouse liver fibrosis by the protein kinase inhibitor sorafenib. *J Autoimmun.* 2013;46:25–34.
39. Pang M, Ma L, Gong R, et al. A novel STAT3 inhibitor, S3I–201, attenuates renal interstitial fibroblast activation and interstitial fibrosis in obstructive nephropathy.

Kidney Int. 2010;78:257–268.
40. Lu K, Chen N, Zhou XX, et al. The STAT3 inhibitor WP1066 synergizes with vorinostat to induce apoptosis of mantle cell lymphoma cells. *Biochem Biophys Res Commun.* 2015;464:292–298.
41. Heymann F, Tacke F. Immunology in the liver–from homeostasis to disease. *Nat Rev Gastroenterol Hepatol.* 2016;13:88–110.
42. Litherland GJ, Elias MS, Hui W, et al. Protein kinase C isoforms zeta and iota mediate collagenase expression and cartilage destruction via STAT3- and ERK-dependent c-fos induction. *J Biol Chem.* 2010;285:22414–22425.
43. Wu MH, Tsai YT, Hua KT, Chang KC, Kuo ML, Lin MT. Eicosapentaenoic acid and docosahexaenoic acid inhibit macrophage-induced gastric cancer cell migration by attenuating the expression of matrix metalloproteinase 10. *J Nutr Biochem.* 2012;23:1434–1439.
44. Li C, Iness A, Yoon J, et al. Noncanonical STAT3 activation regulates excess TGF-beta1 and collagen I expression in muscle of stricturing Crohn's disease. *J Immunol.* 2015;194:3422–3431.
45. Liu LJ, Leung KH, Chan DS, Wang YT, Ma DL, Leung CH. Identification of a natural product-like STAT3 dimerization inhibitor by structure-based virtual screening. *Cell Death Dis.* 2014;5:e1293.